Heliyon 5 (2019) e01864

Contents lists available at ScienceDirect

Heliyon

journal homepage: www.heliyon.com

Heliyon

Decay of muons generated by laser-induced processes in ultra-dense hydrogen H(0)

Leif Holmlid [a,*], Sveinn Olafsson [b]

[a] Atmospheric Science, Department of Chemistry and Molecular Biology, University of Gothenburg, SE-412 96, Göteborg, Sweden
[b] Faculty of Physical Sciences, University of Iceland, Reykjavik, Iceland

ARTICLE INFO

Keywords:
Condensed matter physics
Nuclear physics
Particle physics
Quantum fluids
Superfluid
Experimental nuclear physics
Charged particle emission by condensed matter
Nuclear particle phenomenology
Ultra-dense hydrogen
Muon
Meson
Laser-induced Processes

ABSTRACT

This work reports identification of muons by their characteristic life-time of 2.20 μs after laser-induction of their precursor mesons, both kaons $K^{\pm}$ and K_L^0 and pions $\pi^{\pm}$ in ultra-dense hydrogen H(0). The pair-production signal from scattered muons at a metal converter in front of a photo-multiplier detector is observed with its decay. The observed signal intensity is decreased by a metal beam-flag which intercepts the meson and muon flux to the detector. Using D(0), the observed decay time is (2.23 ± 0.05) μs in agreement with the free muon lifetime of 2.20 μs. This signal is apparently due to the preferential generation of positive muons. Using p(0), the observed decay time is in the range 1–2 μs, thus shorter than the free muon lifetime, as expected when the signal is mainly caused by negative muons which interact with matter by muon capture.

1. Introduction

Nuclear processes [1] induced by ns pulsed lasers in ultra-dense hydrogen H(0) and also similar spontaneous nuclear processes [2] were previously shown to generate mesons (both charged and neutral kaons $K^{\pm}$ and K_L^0as well as pions $\pi^{\pm}$) [3, 4, 5], which decay to muons [6]. A novel muon detection method [6] was developed to cope with the requirement of improved and selective methods for muon detection. Recently, an extensive study of the precursor mesons using magnetic deflection was published [7]. Here, further results are presented on the decay of the muons following laser-induced meson generation. An average decay time constant of (2.23 ± 0.05) μs, in agreement with that for free muons [8, 9], is observed in the experiments.

Ultra-dense hydrogen H(0) [10, 11, 12, 13] has been shown to exist in at least two different forms by experiments in the Göteborg group: ultra-dense deuterium D(0) [14, 15] and ultra-dense protium p(0) [16]. Also mixed forms pD(0) have been studied. The interatomic distance of a few pm, normally at 2.3 pm in spin state $s = 2$, has been proven by laser-induced neutral time-of-flight and time-of-flight mass spectrometry studies [14, 15, 16]. Recently, also rotational spectroscopy with a resolution of a few cm^{-1} has been used: this gives the interatomic distances with high precision and with a resolution of a few femtometers in agreement with theory and previous experiments [17]. Due to the short distances between the hydrogen atoms in these materials, laser-induced nuclear reactions can be initiated by relatively weak pulsed lasers with peak intensity of the order of 10^{13} W cm^{-2} [18, 19].

Muon generation and muon beams are of interest at present for several experiments, mainly in experiments using large laboratories like muon storage rings, muon colliders and muon cooling experiments (for example MICE) [20]. In muon spin spectroscopy (μSR, muon spin rotation), low-energy positive muons formed by decay of positive pions are implanted in materials [21]. The bench-top approach that we take here and in our previous studies is likely to give useful results on muon-catalyzed fusion energy production [22, 23]. For such a process, negative muons are needed at large intensities at low cost and with low energy consumption [24]. Our published results on muon generation [1, 2, 6] indicate that such a development is possible. A recent patent [25] summarizes the specific details of the muon generator. Neutron generation from muon-catalyzed fusion was in fact recently reported with this muon generator [26].

* Corresponding author.
E-mail address: holmlid@chem.gu.se (L. Holmlid).

https://doi.org/10.1016/j.heliyon.2019.e01864
Received 17 August 2018; Received in revised form 1 February 2019; Accepted 29 May 2019

2. Background

The material ultra-dense hydrogen H(0) exists in at least two different forms namely ultra-dense protium p(0) [16] and ultra-dense deuterium D(0) [14, 15]. Also mixed pD forms exist. A few different spin states have been found for H(0) from time-of-flight (TOF) and time-of-flight mass spectrometry (TOF-MS) studies, with $s = 1$, 2 and 3 [15, 16]. Recently, spin states $s = 2$, 3, and 4 were studied with a resolution of a few cm^{-1} by rotational spectroscopy in the visible [17, 27]. The spin state determines the interatomic bond distance as $d = 2.9\ r_q\ s^2$, with $r_q = 0.192$ pm (quantum mechanical electron radius [15]). The interatomic distance in the most common form of ultra-dense hydrogen H(0) with $s = 2$ is approximately 2.3 pm [10, 11, 12]. The molecular structure of H(0) is given by chain clusters H_{2N} with N integer, formed by H–H pairs rotating around a common axis [28, 29]. Also small clusters $H_3(0)$ and $H_4(0)$ occur very frequently [13, 27, 30, 31]. The best low-temperature TOF experiments done on clusters of the forms D_3 and D_4 gave 2.15 pm ± 0.02 pm [13] for $s = 2$, while theory gives 2.23 pm [15]. Rotational spectroscopy in $D_{2N}(0)$ gives 2.245 pm ± 0.003 pm for $s = 2$, recalculating from the best data found for $s = 3$ [17]. The density of H(0) is close to 10^{29} cm^{-3} or 100 kg cm^{-3} [10, 11, 12]. H(0) forms thin superfluid layers on metal and metal oxide surfaces [32, 33]. On non-metal surfaces like glass and plastic, a superfluid film is not formed [33]. H(0) is stable on suitable supports for days and weeks in a vacuum [12] and can be detected by the first probing laser pulse in the experiments.

There are many different levels in the theoretical description of these systems: the classical potential energy [1, 15] and the normal one-electron pictures immediately at hand of course give only partial answers concerning the stability and properties of H(0). The best description so far is based on the theory for superfluids and superconductors, especially the description given by Hirsch [34]. Another prediction can be found in the theory for Compton-scale composite particles by Mayer and Reitz [35]. Such small systems are not easily solved or described by any known quantum mechanical method. In some experiments the smallest basic block that needs to be considered is a pair H_2, as part of and coupled to the chain clusters H_{2N}. This entity of four particles with at least two significant spins is the smallest part that can be described approximately as H(0). We do not assume that a complete theoretical description is within close reach, but the experimental results are quite decisive.

Mesons and muons are released from the ultra-dense hydrogen material H(0) by pulsed laser-beam radiation but occur as well due to spontaneous nuclear reactions with no laser. The energy spectra of the muons are studied in three recent publications from our group [1, 2, 6]. Spontaneous muon generation far above the natural background can be detected for weeks after the formation of H(0), if the material is kept in a vacuum. Mesons are observed by direct time-of-flight using flight distances up to two meters [3, 4, 5, 7]. They are identified by their typical decay times in the studies cited. Charged pions $\pi^{\pm}$ at $\tau = 26$ ns as well as long-lived neutral kaons K_L^0 at $\tau = 52$ ns and charged kaons $K^{\pm}$ at $\tau = 12.4$ ns are all observed [3, 4, 5, 7]. See also the experiment in Fig. 1 for decays due to K_L^0 and $K^{\pm}$. Magnetic deflection proves that most laser-ejected particles from H(0) are neutral, thus probably neutral kaons K_L^0. The charged particles ejected are shown by the magnetic deflection to have masses slightly less than unity, thus being kaons and pions [7]. Their velocities are typically 0.75–0.9 c thus relativistic with an energy above 500 MeV u^{-1} [7].

3. Experimental

The experimental setup used for the decay time experiments is shown in Fig. 2 with dimensions. The laser used is a Nd:YAG laser with pulse energy <0.4 J at 1064 nm and pulse length 7 ns with pulse repetition rate 10 Hz. The laser beam was focused with an $f = 50$ mm lens on the H(0) surface layer on a H(0) generator in a small vacuum chamber of 100 mm

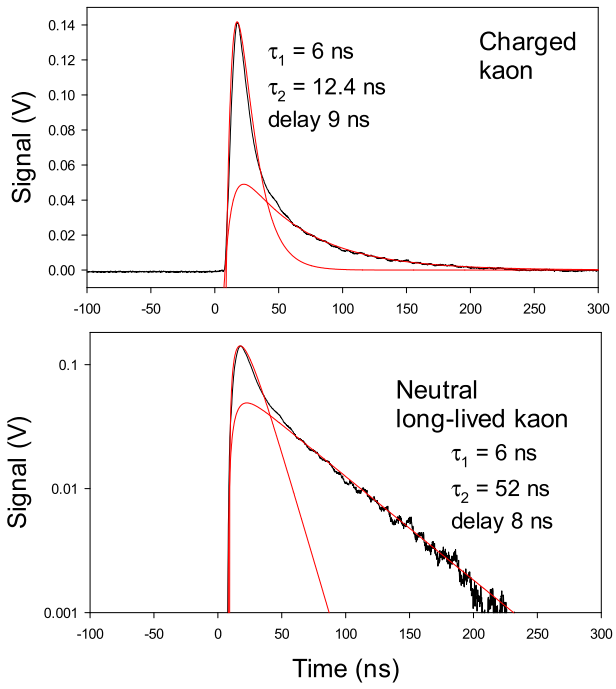

Fig. 1. Time variation of particle signal to an Al foil collector observing muons, instead of the PMT detector in Fig. 2. Oscilloscope measurements, same data in both panels with different vertical axes. The signal pulse has two parts, from charged kaons $K^{\pm}$ at 12.4 ns decay time and neutral long-lived kaons K_L^0 at 52 ns decay time. Linear vertical scale in top panel displays the charged kaon decay and log scale in bottom panel displays the long-lived neutral kaon decay. 0.2 mbar D_2.

diameter and length 1–2 m. The laser beam waist was <20 μm as calculated for a Gaussian beam meaning a laser intensity of $<4 \times 10^{13}$ W cm^{-2}. The experimental behavior and results do not vary with the focusing. Normally, the visible plasma area on the generator surface is a few mm in diameter independent of the laser spot size. In the H(0) generator, several potassium-doped iron oxide catalyst samples [36, 37] form D(0) from deuterium gas (99.8% pure) or p(0) from natural hydrogen gas (99.9995% pure hydrogen, naturally containing only 0.016% D). The ultra-dense material is formed on the upper surface of the H(0) generator. This laser target surface is not rotated. With an H(0) layer on this surface the laser ablation of the metal target is quite weak, and the setup can be used for daily experiments during several weeks with no change in performance. The gas pressure in the chamber is 0.1–10 mbar (Pirani reading uncorrected for gas composition) with or without constant pumping, normally in the lower part of this range if not specially remarked in the figure captions. Since the gas composition is quite complex with large amounts of H(0) clusters, no easy pressure reading correction is possible.

The particle signal is measured with a detector consisting of a plastic scintillator (PS) used as vacuum window [38], an Al converter [6] and a photomultiplier (PMT). The Al converter is normally at a distance of 75 cm from the H(0) generator. It consists of a piece of 20 μm thick Al foil folded and compressed by hand to a mm-thick clump with around five layers of foil. A pinhole free Al foil of thickness 20 μm is mounted in front of the PS giving a light-tight enclosure and no scattered visible light photons (laser light) to the PMT. The PMT is an Electron Tubes 9128B with single electron rise time of 2.5 ns, electron transit time 30 ns, end-window cathode, and linear focused dynode structure. The dark count rate is 100 Hz according to the manufacturer. The Al converter gives high-energy electrons to the PMT by a few different processes [6, 39, 40], mainly by pair production. PMT high voltage is normally 1600 V. The PMT is mounted outside the vacuum in a light-tight metal container. Thus penetration of He atoms formed by any nuclear processes in the

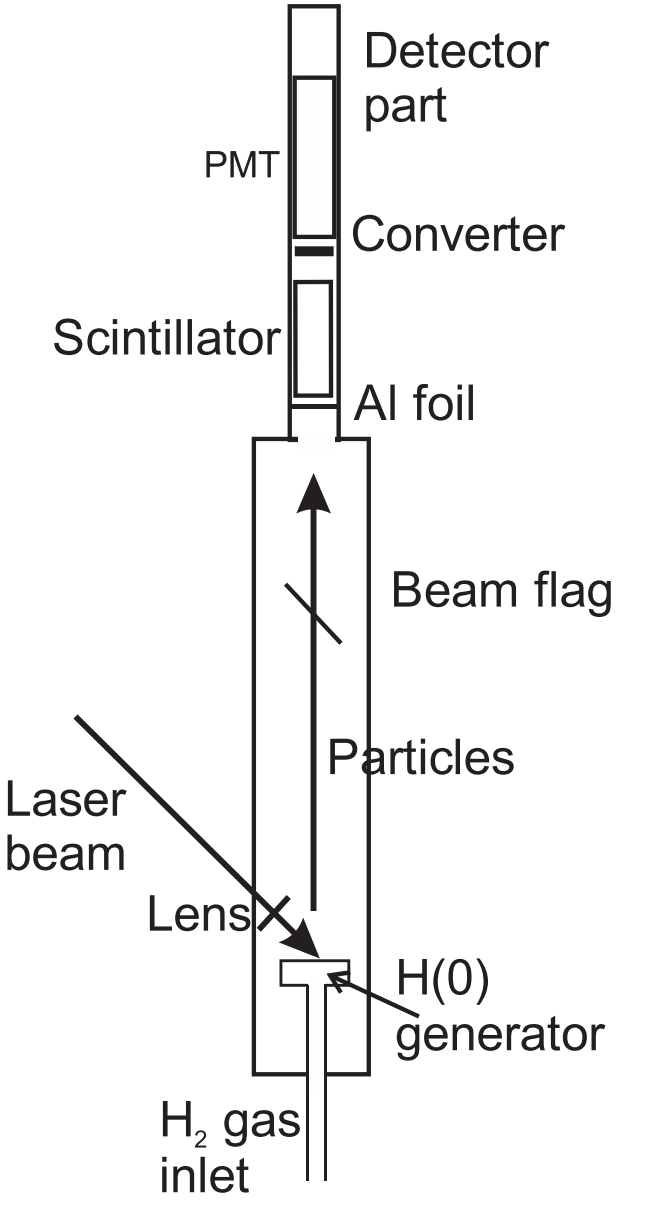

Fig. 2. Principle of the apparatus used, vertical cut. The inner diameter of the tube is 100 mm and the distance between generator and converter is 75 cm.

apparatus into the PMT is prevented and there will be no He pressure at the external PMT.

The signal current from the PMT is taken out via a short 50 Ω coaxial cable to the 50 Ω input of a fast digital two-channel oscilloscope (Tektronix TDS 3032, 300 MHz, 1.2 ns risetime). A 50 Ω RF attenuator is used in the case of off-screen signals to give a factor of nine (-20 dB) lower signal on the oscilloscope. A multi-channel scaler (MCS) with 5 or 20 ns dwell time per channel is used for the pulse counting decay time constant measurements (EG&G Ortec Turbo-MCS). Each MCS spectrum consists of the sum from 1000-5000 laser shots. A preamplifier (Ortec VT120A) with bandwidth 10–350MHz and gain 200 is used for the MCS measurements. A single discriminator level is used in the Turbo-MCS. Since the pulse count time distributions are measured with an Al foil in front of the PMT as also in the MCA energy spectra, the signal is not caused by visible photons from the scintillator into the PMT but by electrons and positrons from pair-production by the fast muons. This means that any scintillator-internal decay process giving photons in the scintillator cannot generate the signal observed.

A beam-flag can be rotated to vertical or horizontal orientation, as indicated in Fig. 2. It is a 1.5 mm thick Al plate at a distance of 64 cm from the H(0) generator. When rotated to the vertical orientation, it allows passage of most of the particles from the generator to the detector [4]. Positive muons and neutral kaons will pass through the beam-flag while the charged precursor kaons and pions will mainly be blocked.

4. Results

4.1. Principle of the experiment

To observe the muon decay directly, the detector or collector should in principle be placed at a large distance from the generator, so that the muons can decay to electrons or positrons at or before reaching the detector. Such a detector would also need to distinguish between the decay leptons from muons and from their precursor mesons. Due to the broad electron energy distributions from the muon decay, this principle is rather difficult to use in a setup which generates meson showers of the complexity which is seen here. (Alternatively, the detector needs to be selective to muons [6]). Further, if the muons move with a velocity close to *c*, the distance to the detector should be more than several hundred meters. In general, the muons may move through matter without strong ionization [39]. However, since the muons with the kinetic energy observed here scatter in the laboratory equipment and in the surrounding walls, a decaying muon cloud exists in the laboratory after the laser pulse. Of special interest are the scattering properties of a layer of H(0) [19, 29]. Such a layer reflects charged particles even at high energy, due to the extreme density of this layer. This means that muons may have their final scattering interaction at such a layer on the target before moving to the detector.

The negative muons may be captured [40] after collisional deceleration and may have a shorter lifetime than free muons [8]. Positive muons will only scatter with energy loss and cannot be captured and will thus more likely display the free muon lifetime. The muons interact with the converter at the PMT mainly by pair production, giving electron - positron pairs which can be detected by the PMT detector, before they decay (submitted). Thus, the density of the positive muon cloud around the apparatus will decay correctly with the free muon lifetime, after the laser pulse forms the precursor mesons which have relatively short lifetimes. If the positive muons initially have high kinetic energy, their observed lifetime will be longer than the stationary free lifetime of 2.20 μs [8] due to relativistic effects. If the rate of electron-positron pair--production varies appreciably with the kinetic energy of the muons, non-exponential decays may be found. Since the decay time distributions are measured with an Al foil in front of the PMT as in the MCA energy spectra, the signal is not caused by visible photons from the scintillator but by electrons and positrons. This means that any internal decay process giving photons in the scintillator used cannot generate the signal observed.

Thus, a direct measurement of the free muon decay-time requires that mainly positive muons can be created, since such muons will not interact too much with materials, and will not be captured by the nuclei in the materials even if they thermalize. However, the muons should probably not be allowed to decelerate too much by collisions, since then the pair-production rate decreases appreciably. The electrons and positrons released by the positive muons at the detector during their passage there will be easily observed by the detector as in previous studies [1, 2, 6]. Thus, a method exists for observing the free decay of positive muons released from the H(0) generator.

4.2. Meson decay to muons

The laser pulse gives emission of mesons, both kaons and pions [4, 5, 7], from the H(0) generator. When a metal foil collector is mounted at a distance of 1–2 meters as in these references, the signal to the collector shows one or a few intermediates. One example is given in Fig. 1. It shows in this case two intermediates in a decay chain, with a rise time close to

the laser pulse rise time and a decay time typical for the mesons formed, in this case charged kaons $K^{\pm}$ and neutral long-lived kaons K_L^0. Extensive studies [4, 5, 7] show that the kaons and pions ejected from the generator are relatively slow and decay to muons before reaching the collector. These muons are normally the particles which give the signal current in these studies by impinging on the collector foil, and the signal decay is due to the disappearance of the mesons after the laser pulse has ended. This means that the decay times of the mesons can be determined accurately, and a relativistic increase of the decay time is not normally observed. Thus, the signal decays with a time constant of 12–52 ns due to the meson decay. This shows directly that mesons are generated by the laser impact and it can safely be concluded that muons are formed by the meson decay within approximately 100 ns.

4.3. Muon MCA spectra

Energy MCA spectra due to muons show that the muon interaction with matter is mainly electron-positron pair production. Such spectra have been measured with a similar PMT detector with a converter in front of the PMT cathode [2, 6]. The converter is made from Al foil or other solid material [2, 6]. The distance from the H(0) generator is up to 5 m in air, and 1–2 m in vacuum. One example is shown in Fig. 3. The bottom panel in the figure shows the MCA data in the form of a Kurie plot [1, 2, 6]. The calibration of the energy scale used ^{137}Cs beta electrons at 513 keV [1, 2, 6]. The MCA spectra do not vary with the direction of the detector in the laboratory, but vary slightly in intensity with detector position in the laboratory, normally being higher at larger distance from the H(0) generator. Thus, the particles detected are muons which scatter freely, even elastically, in the laboratory environment.

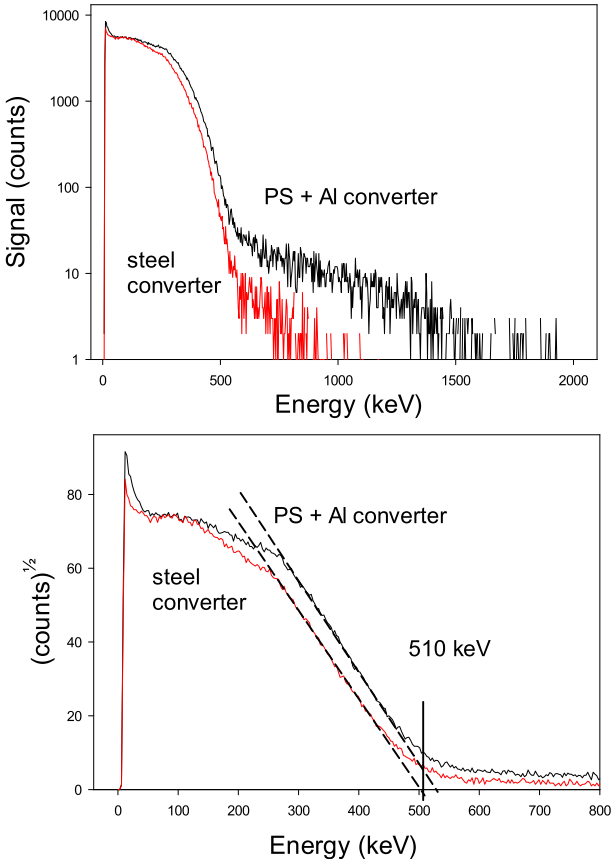

Fig. 3. MCA spectra showing muon detection by pair-production with maximum energy around 510 keV in one experiment. Same data plotted with two different vertical scales, log scale in the top panel to show the overall appearance and square root of counts in the bottom panel to give a Kurie-like plot with a linear part to the energy cut-off. Energy calibration used ^{137}Cs beta electrons at 513 keV [1, 2, 6]. Red curves use only a steel plate converter, black curves use PS + Al converter as in Fig. 2. H_2 at 0.1 mbar.

4.4. Signal decay

Pulse count time distributions or MCS spectra with the PMT at the top of the apparatus as in Fig. 2 show a time variation as a decay of the signal after the laser pulse interacted with the H(0) layer. This decay is due to the decreasing number of muons in the cloud at the apparatus. The decay is exponential and often close to the known decay-time of muons at 2.20 μs. It varies between a factor of two shorter than this value and slightly longer, as expected due to muon capture processes as the cause of the shorter times, and relativistic velocity of the muons as the cause of the longer times. An example of the decay observed with D(0) in the source is shown in Fig. 4. The calculated curve there is an exponential with decay time (2.04 ± 0.04) μs. Note that this is data taken with the Al pillow in front of the cathode, thus with mainly leptons to the PMT and no light from the scintillator. The fitted decay time constants are given at convergence, using the non-linear Marquardt-Levenberg fit procedure in the program SigmaPlot 13. The error limits are the standard errors given by this program.

4.5. Beam flagging

The signal intensity to the detector in the decay time experiments is strongly influenced by the beam flag shown in Fig. 2. This is shown in Fig. 5 in an experiment with p(0) in the generator and short decay time close to 1.4 μs, thus probably mainly with negative muons. In this case, the signal with the flag closed is strongly decreased and does not have an obvious exponential decay. Of course, with mainly negative muons on their way from the target to the converter, they are expected to interact with the thick beam flag and they may be scattered more strongly than positive muons are.

When instead D(0) is used a longer decay time close to 2.2 μs is observed and the beam flag does not decrease the signal as much as in the case above with p(0). This case is shown in Fig. 6. In this case as assumed with mainly positive muons, the interaction with the beam flag is smaller and more of the muons may pass through it. Of course, the energy of the muons may also be slightly different from the case in Fig. 5 for other reasons, so that the transmission through the flag is different.

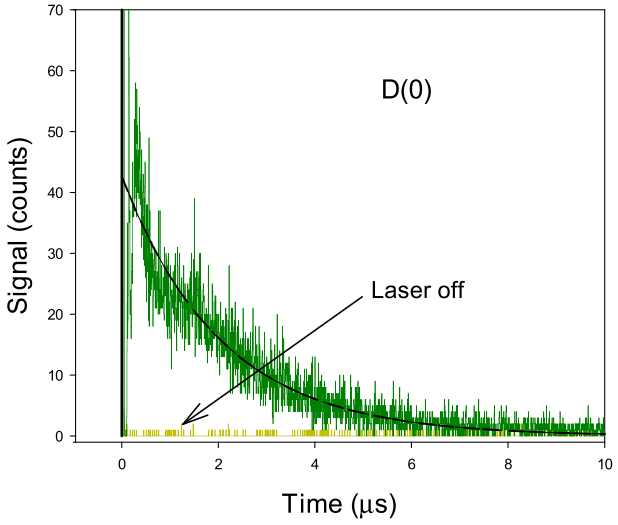

Fig. 4. Laser-induced pulse counting MCS decay signal with D(0). Decay time (2.22 ± 0.03) μs in range 0.9–10 μs in separate fit. SigmaPlot 13 was used for the fit. 1000 shots per spectrum, 5 ns dwell time. PS and Al converter. The spectrum at the bottom is found with laser off.

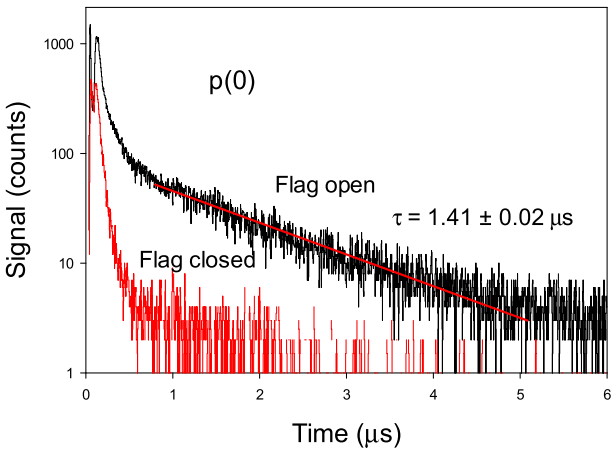

Fig. 5. Laser-induced pulse counting MCS signal from p(0), with open and closed beam-flag. Dwell-time 5 ns, 5000 shots per spectrum. PS and Al converter. 0.3 mbar H_2.

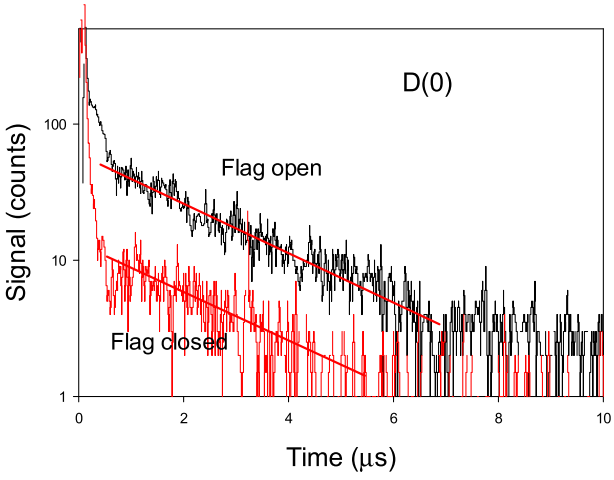

Fig. 6. Laser-induced pulse counting MCS signal from D(0), with open and closed beam-flag. Dwell-time 20 ns, 1000 shots per spectrum. PS and Al converter.

There are also other factors which may influence the interpretation of the experiments with beam flagging. In all experiments, the beam flag can remove the major part of the signal. This indicates that the signal observed originates from below in the chamber, from the source region. If the decaying muons have stayed in the vicinity through several scattering events before they pass to the detector region and give the electron-positron pairs which are detected, they could be thought to arrive from arbitrary directions, not only from the source region. However, their last scattering event before passing close to the detector is likely to be somewhere in the structure of the vacuum chamber, for example on the walls and at the source which parts are covered by an ultra-dense hydrogen H(0) layer. Such layers give very efficient scattering for various particles, as is observed directly in previous experiments [19, 29].

Other experiments with beam flagging [1] conclude that the particles blocked by the beam flag are not muons but rather their precursor mesons. In these experiments, the MCA energy spectra showed that high energy particles were removed by the beam flag, but that the normal muon signal at lower energy (due to pair production) was not influenced by the flag. Such a case is shown in Fig. 7. As can be seen in Fig. 5, this signal at short times (where the meson signal exists) is also in the present case strongly decreased by the beam flag. Thus, these results show that the direct meson signal at short times as well as the muon signal at longer

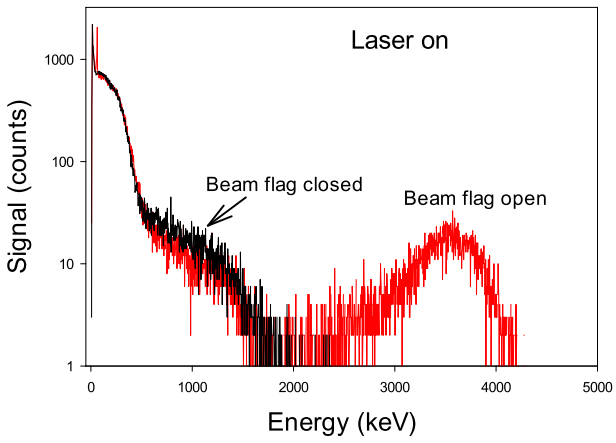

Fig. 7. Beam flag effect on MCA signal. Energies up to 4 MeV (^{137}Cs beta electron calibration) are observed with beam flag open. Signal of mesons and muons. PS and Al converter. < 0.1 mbar D_2.

times (which is studied here) are decreased by the beam flag.

4.6. Decay time measurements

A nice decay from the MCS measurements with D(0) in the muon generator is shown in Figs. 6 and 8. The single time constant appears clearly at approximately 2.3 μs, close to the decay time for free muons. In Fig. 8 the measured points and the least-squares fitted exponential curve are shown. The program used for the fit was Sigma-Plot 13 using a model with one exponential decaying term. The measured lifetime of 2.33 μs ± 0.08 μs is slightly larger than the best muon life-time value of 2.196981 μs [8]. By combining this measured value with the result in Fig. 4, a better value of (2.28 ± 0.04) μs is obtained. This measured decay time is longer than the best lifetime of 2.20 μs. If this longer lifetime observed here is due to a relativistic effect, it corresponds to a relatively low average kinetic energy of 3.8 MeV for the muon during its decay time. Since some muons may receive an initial kinetic energy of several hundred MeV [7], this indicates that the energy loss to the apparatus materials is relatively fast, probably taking less than 1 μs [23]. The background without laser is approximately 0.2 counts per channel, insignificant relative to the signal studied, as shown in Fig. 4. These results show directly that the decay process is due to particles created by the laser pulse at the generator and that these particles are scattered in the apparatus. Such a long time constant cannot be due to gamma photons from the laser-induced plasma, which decays in approximately 20 ns as observed by collectors in Refs. [4, 5].

The measured decay time should be corrected slightly by subtracting the average meson lifetime from the total time observed after the laser pulse. The most common meson observed is the long-lived neutral kaon $K_L^0$with lifetime 51–52 ns from hundreds of experiments (with one example in Fig. 1) giving this as the most common meson decay time in the experiments. This type of meson decays to charged pions and muons, and the pions also give muons after a decay time of 26 ns. This means that the final result for the of muon lifetime after subtracting 52 ns here is (2.23 ± 0.05) μs, where the error limit is increased slightly due to possible contributions from other precursor mesons. This gives the final value found here into agreement with the best value of the muon lifetime [8] within the error limits.

Using p(0) instead of D(0) normally gives shorter decay times, often closer to 1.5 μs with one example in Fig. 5. This indicates that positive muons are fewer in this case and that as expected the decay-time of negative muons is shortened due to interaction of the muons with matter [40]. This implies that mainly negative muons reach the converter in this case. These decay results confirm that muons are due to the laser-induced processes in H(0) as concluded previously from the energy spectra [2, 6].

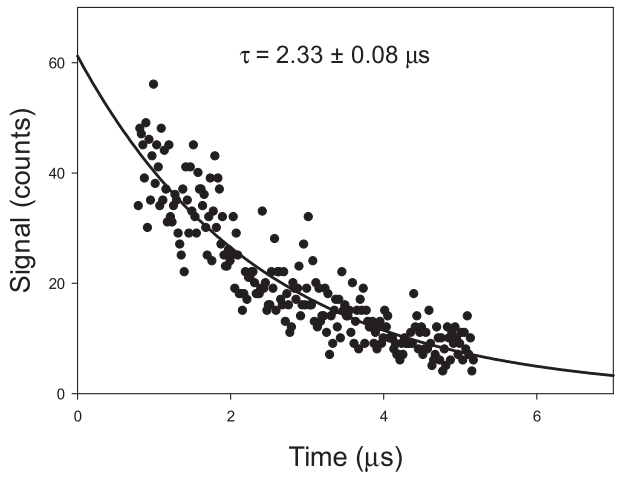

Fig. 8. Least-squares fitted exponential and data points from curve with beam-flag open in fig. 6. Decay time (2.33± 0.08) μs in range 0.8 - 5.2 μs. SigmaPlot 13 was used for the fit.

5. Discussion

The particle signals observed here are clearly caused by laser-induced nuclear processes in H(0). A few steps in these processes have been identified. The first one is the laser-induced transfer of the $H_2(0)$ pairs in H(0) from excitation state $s = 2$ (with 2.3 pm H–H distance) to $s = 1$ (at 0.56 pm H–H distance) [15]. The state $s = 1$ may lead to a fast nuclear reaction, and the internuclear distance for $s = 1$ is in fact similar to that known to give muon catalyzed fusion with a high rate within a few ns [23]. The nuclear process may involve two protons. The first particles observed after a short distance [3, 4, 5, 7] are indeed kaons, both neutral and charged, but the initial formation also of pions cannot be excluded completely. From the six quarks in the two protons, three kaons may be formed. Two protons have a mass of 1.88 GeV while three kaons have a mass of 1.49 GeV. Thus, the reaction 2 p → 3 K releases 390 MeV, thus around 130 MeV per kaon on average. The kaons formed decay to pions within 52 ns and then to muons.

The difference between the results using D(0) and p(0) needs to be discussed. From several experiments, it seems likely that positive kaons are formed at lower density of H(0), while negative kaons are formed preferentially at higher density. In the present experiments, that should mean that positive muons should be formed using D(0), since the signal in Figs. 5 and 6 is slightly lower for D(0). This agrees with the conclusion that D(0) here gives more positive muons and thus a time constant close to the free muon decay. The reason for this density effect is however not obvious. One might speculate that in D(0) only every second nuclei is a proton, and thus that the 2 p → 3 K transition is less likely, but this does not give any clue to why positive muons should be formed more often in that case. Another possibility would be that at high density, neutral kaons are formed preferentially and at low density, charged kaons are more common. However, charge asymmetry is required to explain the observations in such a case.

6. Conclusions

The laser-induced pulsed signal previously concluded to be due to muons is now found to have a decay time constant in the expected range 1.0–2.3 μs. The best known decay time for free muons is 2.20 μs, and the measured decay time of (2.23 ± 0.05) μs from D(0) is concluded to be due to positive muons. Using p(0), the decay time is shorter than 2.2 μs as expected for negative muons due to their more intense interaction with matter (muon capture).

Declarations

Author contribution statement

Leif Holmlid: Conceived and designed the experiments; Performed the experiments; Analyzed and interpreted the data; Wrote the paper.

Sveinn Olafsson: Conceived and designed the experiments; Analyzed and interpreted the data; Wrote the paper.

Funding statement

This work was supported by GU Ventures AB, The Holding Company at University of Gothenburg.

Competing interest statement

The authors declare no conflict of interest.

Additional information

No additional information is available for this paper.

Acknowledgements

Part of the equipment was constructed and built with support from GU Ventures AB, The Holding Company at University of Gothenburg. LH thanks his wife, Ulla Holmlid, for help with checking the proof.

References

[1] L. Holmlid, S. Olafsson, Charged particle energy spectra from laser-induced processes: nuclear fusion in ultra-dense deuterium D(0), Int. J. Hydrogen Energy 41 (2016) 1080–1088.
[2] L. Holmlid, S. Olafsson, Spontaneous ejection of high-energy particles from ultra-dense deuterium D(0), Int. J. Hydrogen Energy 40 (2015) 10559–10567.
[3] L. Holmlid, MeV particles in a decay chain process from laser-induced processes in ultra-dense deuterium D(0), Int. J. Mod. Phys. E 24 (2015) 1550026.
[4] L. Holmlid, Nuclear particle decay in a multi-MeV beam ejected by pulsed-laser impact on ultra-dense hydrogen H(0), Int. J. Mod. Phys. E 24 (2015) 1550080.
[5] L. Holmlid, Leptons from decay of mesons in the laser-induced particle pulse from ultra-dense protium p(0), Int. J. Mod. Phys. E 25 (2016) 1650085.
[6] L. Holmlid, S. Olafsson, Muon detection studied by pulse-height energy analysis: novel converter arrangements, Rev. Sci. Instrum. 86 (2015), 083306.
[7] L. Holmlid, Mesons from laser-induced processes in ultra-dense hydrogen H(0), PLoS One 12 (1) (2017), e0169895.
[8] Particle Data Group, C. Amsler, M. Doser, M. Antonelli, D.M. Asner, K.S. Babu, et al., Review of particle physics, Phys. Lett. B 667 (2008) 1. URL: http://pdg.lbl.gov.
[9] W.E. Burcham, M. Jobes, Nuclear and Particle Physics, Pearson, Harlow, 1995.
[10] S. Badiei, P.U. Andersson, L. Holmlid, Laser-induced variable pulse-power TOF-MS and neutral time-of-flight studies of ultra-dense deuterium, Phys. Scripta 81 (2010), 045601.
[11] P.U. Andersson, L. Holmlid, Deuteron energy of 15 MK in a surface phase of ultra-dense deuterium without plasma formation: temperature of the interior of the Sun, Phys. Lett. A 374 (2010) 2856.
[12] S. Badiei, P.U. Andersson, L. Holmlid, Production of ultra-dense deuterium, a compact future fusion fuel, Appl. Phys. Lett. 96 (2010) 124103.
[13] L. Holmlid, High-charge Coulomb explosions of clusters in ultra-dense deuterium D(-1), Int. J. Mass Spectrom 304 (2011) 51.
[14] S. Badiei, P.U. Andersson, L. Holmlid, High-energy Coulomb explosions in ultra-dense deuterium: time-of-flight mass spectrometry with variable energy and flight length, Int. J. Mass Spectrom. 282 (2009) 70.
[15] L. Holmlid, Excitation levels in ultra-dense hydrogen p(-1) and d(-1) clusters: structure of spin-based Rydberg Matter, Int. J. Mass Spectrom. 352 (2013) 1.
[16] L. Holmlid, Laser-mass spectrometry study of ultra-dense protium p(-1) with variable time-of-flight energy and flight length, Int. J. Mass Spectrom. 351 (2013) 61.
[17] L. Holmlid, Emission spectroscopy of IR laser-induced processes in ultra-dense deuterium D(0): rotational transitions with spin values s = 2, 3 and 4, J. Mol. Struct. 1130 (2017) 829–836.
[18] P.U. Andersson, L. Holmlid, Fusion generated fast particles by laser impact on ultra-dense deuterium: rapid variation with laser intensity, J. Fusion Energy 31 (2012) 249–256.
[19] F. Olofson, L. Holmlid, Time-of-flight of He ions from laser-induced processes in ultra-dense deuterium D(0), Int. J. Mass Spectrom. 374 (2014) 33.
[20] M. Bogomilov, Y. Karadzhov, D. Kolev, I. Russinov, R. Tsenov, G. Vankova-Kirilova, L. Wang, F.Y. Xu, S.X. Zheng, R. Bertoni, et al., The MICE muon beam on ISIS and

the beam-line instrumentation of the muon ionization cooling experiment, J.Instrumentation 7 (2012).
[21] E. Morenzoni, F. Kottmann, D. Maden, B. Matthias, M. Meyberg, Th. Prokscha, Th. Wutzke, U. Zimmermann, Generation of very slow polarized positive muons, Phys. Rev. Lett. 72 (1994) 2793.
[22] L.W. Alvarez, H. Bradner, F.S. Crawford Jr., J.A. Crawford, P. Falk-Vairant, M.L. Good, J.D. Gow, A.H. Rosenfeld, F. Solmitz, M.L. Stevenson, H.K. Ticho, R.D. Tripp, Catalysis of nuclear reactions by μ mesons, Phys. Rev. 105 (1957) 1127.
[23] D.V. Balin, V.A. Ganzha, S.M. Kozlov, E.M. Maev, G.E. Petrov, M.A. Soroka, G.N. Schapkin, G.G. Semenchuk, V.A. Trofimov, A.A. Vasiliev, A.A. Vorobyov, N.I. Voropaev, C. Petitjean, B. Gartner, B. Lauss, J. Marton, J. Zmeskal, T. Case, K.M. Crowe, P. Kammel, F.J. Hartmann, M.P. Faifman, High precision study of muon catalyzed fusion in D_2 and HD gas, Phys. Part. Nucl. 42 (2011) 185.
[24] L. Holmlid, Existing source for muon-catalyzed nuclear fusion can give MW thermal fusion generator, Fusion Sci. Technol. 75 (2019) 208–217.
[25] L. Holmlid, "Apparatus for Generating Muons with Intended Use in a Fusion Reactor". Patent Nr SE 539684 C2, Published, 2017, 10-31.
[26] L. Holmlid, Neutrons from muon-catalyzed fusion and from capture processes in an ultra-dense hydrogen H(0) generator, Fusion Sci. Technol. 74 (2018) 219–228.
[27] L. Holmlid, Rotational emission spectroscopy in ultra-dense hydrogen p(0) and $p_xD_y(0)$: groups p_N, pD_2, p_2D and $(pD)_N$, J. Mol. Struct. 1173 (2018) 567–573.
[28] P.U. Andersson, L. Holmlid, Superfluid ultra-dense deuterium D(-1) at room temperature, Phys. Lett. A 375 (2011) 1344.
[29] P.U. Andersson, L. Holmlid, Cluster ions D_N^+ ejected from dense and ultra-dense deuterium by Coulomb explosions: fragment rotation and D^+ backscattering from ultra-dense clusters in the surface phase, Int. J. Mass Spectrom. 310 (2012) 32.
[30] L. Holmlid, B. Kotzias, Phase transition temperatures of 405-725 K in superfluid ultra-dense hydrogen clusters on metal surfaces, AIP Adv. 6 (2016), 045111.
[31] L. Holmlid, Laser-induced nuclear processes in ultra-dense hydrogen take place in small non-superfluid $H_N(0)$ clusters, J. Clust. Sci. 30 (2019) 235–242.
[32] L. Holmlid, Laser-induced fusion in ultra-dense deuterium D(-1): optimizing MeV particle ejection by carrier material selection, Nucl. Instr. Meth. B 296 (2013) 66–71.
[33] F. Olofson, L. Holmlid, Superfluid ultra-dense deuterium D(-1) on polymer surfaces: structure and density changes at a polymer-metal boundary, J. Appl. Phys. 111 (2012) 123502.
[34] J.E. Hirsch, The origin of the Meissner effect in new and old superconductors, Phys. Scr. 85 (2012), 035704.
[35] F.J. Mayer, J.R. Reitz, Electromagnetic composites at the Compton scale, Int. J. Theor. Phys. 51 (2012) 322–330.
[36] G.R. Meima, P.G. Menon, Catalyst deactivation phenomena in styrene production, Appl. Catal. A 212 (2001) 239.
[37] M. Muhler, R. Schlögl, G. Ertl, The nature of the iron oxide-based catalyst for dehydrogenation of ethylbenzene to styrene 2. surface chemistry of the active phase, J. Catal. 138 (1992) 413.
[38] Saint-Gobain Products, Scintillation Products, Organic Scintillation Materials, 2001, p. 11.
[39] D.E. Groom, N.V. Mokhov, S. Striganov, Muon stopping power and range tables 10 MeV—100 TeV, Atomic Data Nucl. Data Tables 76 (2) (2001) (LBNL-44742).
[40] D.F. Measday, The nuclear physics of muon capture, Phys. Rep. 354 (2001) 243.